N95-10568

# Characteristics of a Dry, Pulsating Microburst at Denver Stapleton Airport.

F. Proctor,

NASA Langley Research Center

[For these Proceedings, the author has furnished three papers:

Influence of Low-Level Environmental Shear on Microburst Structure: Numerical Case Study,

Numerical Simulation of a Pulsating, Low-Reflectivity Microburst Event,

and

Case Study of a Low-Reflectivity Pulsating Microburst: Numerical Simulation of the Denver, 8 July 1989, Storm.

These appear in order on the following pages.]

# INFLUENCE OF LOW-LEVEL ENVIRONMENTAL SHEAR ON MICROBURST STRUCTURE: NUMERICAL SENSITIVITY STUDY

FRED H. PROCTOR

*NASA-LANGLEY RESEARCH CENTER*
Flight Management Division
*HAMPTON, VA 23681-0001*



September 28, 1993

FIFTH COMBINED MANUFACTURERS' AND TECHNOLOGISTS'
WIND SHEAR REVIEW MEETING

# Presentation Outline

I. INTRODUCTION

- A. TASS MODEL DESCRIPTION
- B. INITIAL CONDITIONS

II. RESULTS OF 3-D SENSITIVITY STUDY
AMBIENT SHEAR VS:

- A. PEAK LOW-LEVEL WIND CHANGE
- B. PEAK 1-KM F-FACTOR
- C. PEAK LOW-LEVEL WIND SPEED

III. RESULTS FROM CASE WITH STRONG MULTI-DIRECTIONAL SHEAR

IV. SUMMARY

## Introduction

In previous studies using the two-dimensional axisymmetric version of the Terminal Area Simulation System (TASS) the effect of environmental parameters and other factors was examined for isolated and stationary microbursts (Proctor 1988, 1989). The intensity and structure of the simulated microbursts were strongly affected by the lapse rates of ambient temperature and humidity, as well as the height of the melting level. These experiments, however, were limited to an axisymmetric model framework, and could not allow for an examination of the effects of translation and ambient wind shear.

The present study extends these studies by examining the influence of ambient vertical wind shear on microburst intensity, asymmetry, and translation. This is achieved with the three-dimensional, high-resolution, version of the TASS model, by selectively varying the initial inputs for ambient low-level vertical wind shear and keeping all other input parameters fixed. A similar approach has been used by Weisman and Klemp (1982, 1984) and Weisman (1993) in the study of vertical wind shear on isolated convective cells. Although our study here differs significantly from these studies in that we initially start out with a prescribed precipitation shaft as in Proctor (1988, 1989), rather than trying to simulate the complete storm evolution.

## Numerical Model

Details of the numerical model used in this study have been described by Proctor (1987a), and should be referred to for details. The TASS model is a three-dimensional, time dependent, "cloud" model, with prognostic equations for momentum, pressure, continuity of water substance, and potential temperature. The six coupled equations for continuity of water substance include an equation each for water vapor, cloud droplets, cloud ice crystals, rain, hail or graupel, and snow. The model also includes parameterizations for surface friction and cloud-microphysical interactions. Salient characteristics of the TASS model are listed in table 1, and a list of the cloud microphysical parameterization are given in table 2. The TASS model has been validated against a number of cumulonimbus cases (e.g., Proctor 1987b, 1993; Proctor and Bowles 1992), many of which were associated with intense microburst events.

## Initial Conditions and Description of Experiments

An isolated microburst event is simulated by specifying a distribution of precipitation at the model top boundary and allowing it to fall within an environment conducive to wet microbursts. Twelve numerical experiments are conducted, which assume two precipitation shaft sizes and various ambient wind profiles as will be discussed below.

The dimension of the physical grid domain is 10 km in the west-east direction (x-coordinate), 7.5 km in the south-north direction (y-coordinate), and 5 km in the vertical direction (z-coordinate). The domain is resolved by 32 levels with a vertical grid separation

stretching from 23 m near the ground to 280 m near 5 km. Each level is resolved by 102 x 77 grid points with a uniform horizontal grid spacing of 100 m.

The ambient (initial) profile for temperature and humidity typifies a warm moist wet-microburst environment, and is used for all experiments.

The initial ambient winds are horizontally uniform and are a function of height only. The ambient winds are specified according to:

$$U_e(z) = U_o + U_G\left(\frac{z}{2000}\right)^{0.4} \qquad for\ z < 2000\ m$$

$$U_e(z) = U_o + U_G \qquad for\ z \geq 2000\ m$$

*and,*

$$V_e(z) = V_o$$

where $U_e$ and $V_e$ are the ambient wind components (m/s) in the x and y directions, respectively; and z is the altitude above the ground (m). At the ground (z = 0) the wind velocity is required to be zero in accordance with the no slip surface boundary condition. In all experiments the ambient wind speed and direction are constant above 2000 m. Input values for $U_G$, $U_o$, and $V_o$ are listed for each experiment in Table 3.

For all experiments the type of precipitation prescribed at the top boundary is assumed to be of the hail/graupel class with a size distribution intercept of $2 \times 10^5$ $m^4$. The distribution of precipitation at the top boundary is specified as

$$Q(X,Y) = Q_O\, e^{-(R/\sigma)^3}$$

where

$$R(X,Y) = \sqrt{(X-X_O)^2 + (Y-Y_O)^2}$$

and where $X_O$,$Y_O$ is a center location on the top boundary. For all experiments in this study $Q_O$ is 6 g $m^{-3}$. The input parameter $\sigma$, which controls the radial distribution of the precipitation shaft and ensuing downdraft diameter, is listed for each experiment in Table 3. In all experiments the model grid and precipitation at the top boundary translate with the ambient wind velocity above 2000 m.

**Table 1. Salient Characteristics of TASS 2.4**

| |
|---|
| Compressible, nonhydrostatic equation set |
| Non-Boussinesq formulation for density variations |
| Three-dimensional staggered grid with stretched vertical spacing |
| Movable, storm-centering mesh |
| Explicit time-split, second-order, Adams-Bashforth time differencing and second-order quadratic-conservative space differencing for velocity and pressure |
| Fourth-order quadratic-conservative space differencing and third-order Adams-Bashforth time differencing for temperature and water-vapor |
| Third-order time/space differencing with upstream-biased quadratic interpolation for liquid and frozen water substance equations |
| Nonreflective radiation boundary conditions applied to open lateral boundaries |
| Filter and Sponge applied to top four rows in order to diminish gravity wave reflection at top boundary |
| No explicit numerical filtering applied to interior points |
| Surface friction layer based on Monin-Obukhov Similarity theory |
| Smagorinsky subgrid-turbulence closure with Richardson number dependence |
| Liquid and ice-phase microphysics |
| Inverse-exponential size distributions assumed for rain, hail/graupel, and snow |
| Raindrop intercept function of amount of rainwater |
| Snow treated as spherical, low-density graupel-like snow particles |
| Wet and dry hail growth |
| Accumulated precipitation advected opposite of grid motion, so as to remain ground relative |
| Radar reflectivity diagnosed from model rain, snow, and hail/graupel fields |

| Table 2. Cloud Microphysical Interactions |
| --- |
| Accretion of cloud droplets by rain |
| Condensation of water vapor into cloud droplets |
| Berry-Reinhardt formulation for autoconversion of cloud droplet water into rain |
| Evaporation of rain and cloud droplets |
| Spontaneous freezing of supercooled cloud droplets and rain |
| Initiation of cloud ice crystals |
| Ice crystal and snow growth due to riming |
| Vapor deposition and sublimation of hail/graupel, snow, and cloud ice crystals |
| Accretion by hail/graupel of cloud droplets, cloud ice crystals, rain, and snow |
| Contact freezing of supercooled rain resulting from collisions with cloud ice crystals or snow |
| Production of hail/graupel from snow riming |
| Melting of cloud ice crystals, snow, and hail/graupel |
| Shedding of unfrozen water during hail wet growth |
| Shedding of water from melting hail/graupel and snow |
| Conversion of cloud ice crystals into snow |
| Accretion by snow of cloud droplets, cloud ice crystals, and rain |
| Evaporation or vapor condensation on melting hail/graupel and snow |

**TABLE 3. Input variables for each experiment**

| RUN # | $U_G$ (m/s) | $U_o$ (m/s) | $V_o$ (m/s) | $\sigma$ (m) | $\Delta U_e$ (m/s) | FILE |
|---|---|---|---|---|---|---|
| 1 | 0.0 | 0 | 0 | 750 | 0.0 | 05a |
| 2 | 5.0 | 0 | 0 | 750 | 4.2 | 09a |
| 3 | 12.5 | 0 | 0 | 750 | 10.4 | 08a |
| 4 | 17.5 | 0 | 0 | 750 | 14.6 | 10a |
| 5 | 25.0 | 0 | 0 | 750 | 20.8 | 06a |
| 6 | 0.0 | 17.5 | 0 | 750 | 0.0 | 20a |
| 7 | 17.5 | 0 | 8.75 | 750 | 14.6 | 19a |
| 8 | 0.0 | 0 | 0 | 1350 | 0.0 | 15a |
| 9 | 5.0 | 0 | 0 | 1350 | 4.2 | 13a |
| 10 | 12.5 | 0 | 0 | 1350 | 10.4 | 12a |
| 11 | 17.5 | 0 | 0 | 1350 | 14.6 | 11a |
| 12 | 25.0 | 0 | 0 | 1350 | 20.8 | 14a |

Values for the input parameters of the 12 experiments are listed in Table 3. As indicated by the value assumed for $\sigma$, experiments 1-7 represent the small-diameter downdraft cases, while experiments 8-12 represent the large-diameter cases. The parameter $\Delta U_e$ represents the vertical change in ambient wind from the lowest model level (at z = 23 m) to the gradient level located at 2000 m, and thus is an indicator of the magnitude of ambient vertical shear. The ambient shear vector is directed eastward in all experiments (except Run #: 1, 6, and 8 which have no shear), and varies in magnitude between each experiment. However, as in Run 7, the ambient wind vector may not always be in the same direction as the shear vector. The sensitivity of the microburst to ambient wind shear is examined by comparing the results between each of the simulations.

## Results

Sensitivity of key microburst parameters to environmental shear are shown in the following three line plots. The tendencies of both the small and large diameter microburst were similar and thus only results from the small diameter microburst are shown in the first two plots.

The plot of ambient vertical shear vs peak velocity differential shows that increasing ambient shear reduces the peak velocity differential of a microburst. More importantly though, the peak velocity differential that is orthogonal to the ambient shear vector (e.g. $\Delta V$ along north-south segments) are less affected by increasing shear than the velocity differential along the shear vector (e.g. $\Delta V$ along east-west segments). Asymmetry of the microburst outflow field is indicated the by the difference in magnitude between the E-W and N-S segments. [For an axisymmetric outflow the peak E-W $\Delta V$ is equal to the peak N-S $\Delta V$.] The results show that asymmetry of the outflow velocity field increases with increasing ambient shear.

The second line plot shows the sensitivity of peak Fbar (1-km averaged F-Factor) at 280 m AGL. As described in Proctor and Bowles (1992) and Switzer et al (1993), values for F-factor are computed assuming horizontal north-south (or east-west) trajectories with an assumed air speed of 75 m/s. Similar to the peak $\Delta V$ curves in the previous plot, peak Fbar along segments orthogonal to the shear vector are stronger than the peak values along segments parallel to the shear vector, with widening differences as the magnitude of shear increases. But unlike in the previous plot, an optimal value occurs for Fbar along segments orthogonal to the shear vector. This optimal value happens for the north-south Fbar when the magnitude of the ambient shear is approximately 15 m/s.

The third plot show the sensitivity of peak outflow speed (ground relative) for both large and small diameter microbursts. The peak outflow speed indicates the severity of the microburst in terms of its potential for inducing damage due to high winds. Our set of experiments indicates that the highest wind speeds occur for an optimal ambient vertical shear of about 15 m/s for both large and small diameter microbursts. The simulations indicate that this peak horizontal wind speed occurs on the downshear side of the microbursts.

The last series of plots show cross sections from a case with strong ambient shear. The plots show radar reflectivity and velocity fields from Run 7 at a time near peak intensity. The ambient shear vector is directed east, although the storm is translating toward the east-northeast (see table 3). The figures show that the outflow is elongated E-W along the shear vector. The horizontal cross section of radar reflectivity at low levels shows a bow-echo shape with maximum radar reflectivity located on the downshear side of the outflow. The east-west vertical cross section shows a strong vortex circulation on the downshear side, which is associated with strong surface-level winds. Such a microburst as in this simulation, may be referred to as what Fujita (1985) calls a "rotor microburst."

## SUMMARY AND DISCUSSION

These results show that microburst asymmetry is influenced by the magnitude of the low-level ambient vertical shear. The microburst outflow elongates in the direction of the shear vector (which is not necessarily in the direction of translation), and generates the greatest hazard (for commercial jet transports) along paths orthogonal to the shear vector. The model results also show that the asymmetry increases with increasing shear magnitude. One implication of these results concerns the detection of a microburst by a ground-based doppler systems. These systems may underestimate the hazard for landing and departing aircraft that are on trajectories orthogonal to both the sensor beam and shear vector, especially if the magnitude of the shear is large. Another implication is that microburst are more likely to be asymmetrical in regions (seasons) where there is climatologically a significant low-level shear.

The model results also show that rotor microbursts and severe wind damage can be a product of the microburst interaction with strong ambient wind shear.

## REFERENCES


*Fujita, T. T., 1985: The Downburst, Microburst and Macroburst. University of Chicago Press, 122 pp.*

*Proctor, F. H., 1987a: The Terminal Area Simulation System. Volume I: Theoretical formulation. NASA Contractor Rep. 4046, NASA, Washington, DC, 176 pp. [Available from NTIS]*

*Proctor, F. H., 1987b: The Terminal Area Simulation System. Volume II: Verification Experiments. NASA Contractor Rep. 4047, NASA, Washington, DC, 112 pp. [Available from NTIS]*

*Proctor, F. H., 1988: Numerical simulations of an isolated microburst. Part I: Dynamics and structure. J. Atmos. Sci., 45, 3137-3160.*

*Proctor, F. H., 1989: Numerical simulations of an isolated microburst. Part II: Sensitivity experiments. J. Atmos. Sci., 46, 2143-2165.*

*Proctor, F. H., 1993: Case study of a low-reflectivity pulsating microburst: numerical simulation of the Denver, 8 July 1989, storm. Preprints, 17th Conf. on Severe Local Storms, St. Louis, Mo., Amer. Meteor. Soc., 677-680.*

*Proctor, F. H., and R. L. Bowles, 1992: Three-dimensional simulation of the Denver 11 July 1988 microburst-producing storm. Meteorol. and Atmos. Phys., 47, 107-124.*

*Switzer, G. F., F. H. Proctor, D. A. Hinton and J. V. Aanstoos, 1993: Windshear database for forward-looking systems certification. NASA TM-109012, 133 pp.*

*Weisman, M. L. and J. B. Klemp, 1982: The dependence of numerically simulated convective storms on wind shear and buoyancy. Mon. Wea. Rev., 110, 504-520.*

*Weisman, M. L. and J. B. Klemp, 1984: the structure and classification of numerically simulated convective storms in directionally varying wind shears. Mon. Wea. Rev., 112, 2479-2498*

*Weisman, M. L., 1993: The genesis of long-lived bow echoes. J. Atmos. Sci., 50, 645-670.*

# TERMINAL AREA SIMULATION SYSTEM (TASS)

*[ALSO KNOWN AS THE NASA WINDSHEAR MODEL]*

- 3-D TIME DEPENDENT EQUATIONS FOR COMPRESSIBLE NONHYDROSTATIC FLUIDS

- PROGNOSTIC EQUATIONS FOR 11 VARIABLES
  1. 3-COMPONENTS OF VELOCITY
  2. PRESSURE
  3. POTENTIAL TEMPERATURE
  4. WATER VAPOR
  5. LIQUID CLOUD DROPLETS
  6. CLOUD ICE CRYSTALS
  7. RAIN
  8. SNOW
  9. HAIL/GRAUPEL
  10. INSECTS

- 1st-ORDER SUBGRID TURBULENCE CLOSURE WITH RICHARDSON NUMBER DEPENDENCY

- SURFACE FRICTION LAYER BASED ON MONIN-OBUKHOV SIMILARITY THEORY

- Choice At LATERAL BOUNDARIES Between OPEN BOUNDARY CONDITIONS ALLOWING MINIMAL REFLECTION or PERIODIC CONDITIONS

- BULK PARAMETERIZATIONS OF CLOUD MICROPHYSICS

# TERMINAL AREA SIMULATION SYSTEM

CAN SIMULATE CONVECTIVE STORMS WITH REASONABLE COMPARISON TO REAL-WORLD EVENTS

- O REQUIRES INPUT VERTICAL PROFILE OF TEMPERATURE, HUMIDITY, WIND SPEED AND DIRECTION, AND ALTITUDE (OR PRESSURE)
- O SOUNDING MUST BE REPRESENTATIVE OF STORM'S ENVIRONMENT
- O SOUNDING MAY BE EITHER OBSERVED, FORECASTED (*e.g. MASS)*, OR INTERPOLATED

SIMULATIONS FROM TASS EXTENSIVELY VALIDATED AGAINST OBSERVED STORMS RANGING FROM

- O SHORT-LIVED WEAK CUMULONIMBUS
- O SEVERE LONG-LASTING SUPERCELL STORMS
- O MICROBURST PRODUCING STORMS
- O HAILSTORMS AND TORNADIC THUNDERSTORMS

# MICROBURST SENSITIVITY TO AMBIENT VERTICAL SHEAR

## *NUMBER OF EXPERIMENTS*

12 NUMERICAL SIMULATIONS:
- O 6 - LEVELS OF AMBIENT VERTICAL SHEAR
- O 2 - MICROBURST DIAMETERS

## *INPUT DATA / ASSUMPTIONS*

PHYSICAL DOMAIN SIZE (3-D)
- O HORIZONTAL (X,Y): 10 KM x 7.5 KM
- O VERTICAL (Z): 5 KM

COMPUTATIONAL RESOLUTION
- O HORIZONTAL - 100 M (102 X 77 GRID POINTS)
- O VERTICAL - 23 M NEAR GROUND STRETCHING TO 280 M AT 5 KM (32 LEVELS)

MICROBURST INITIATED FROM HAIL PRESCRIBED AT TOP BOUNDARY

WET MICROBURST ENVIRONMENT

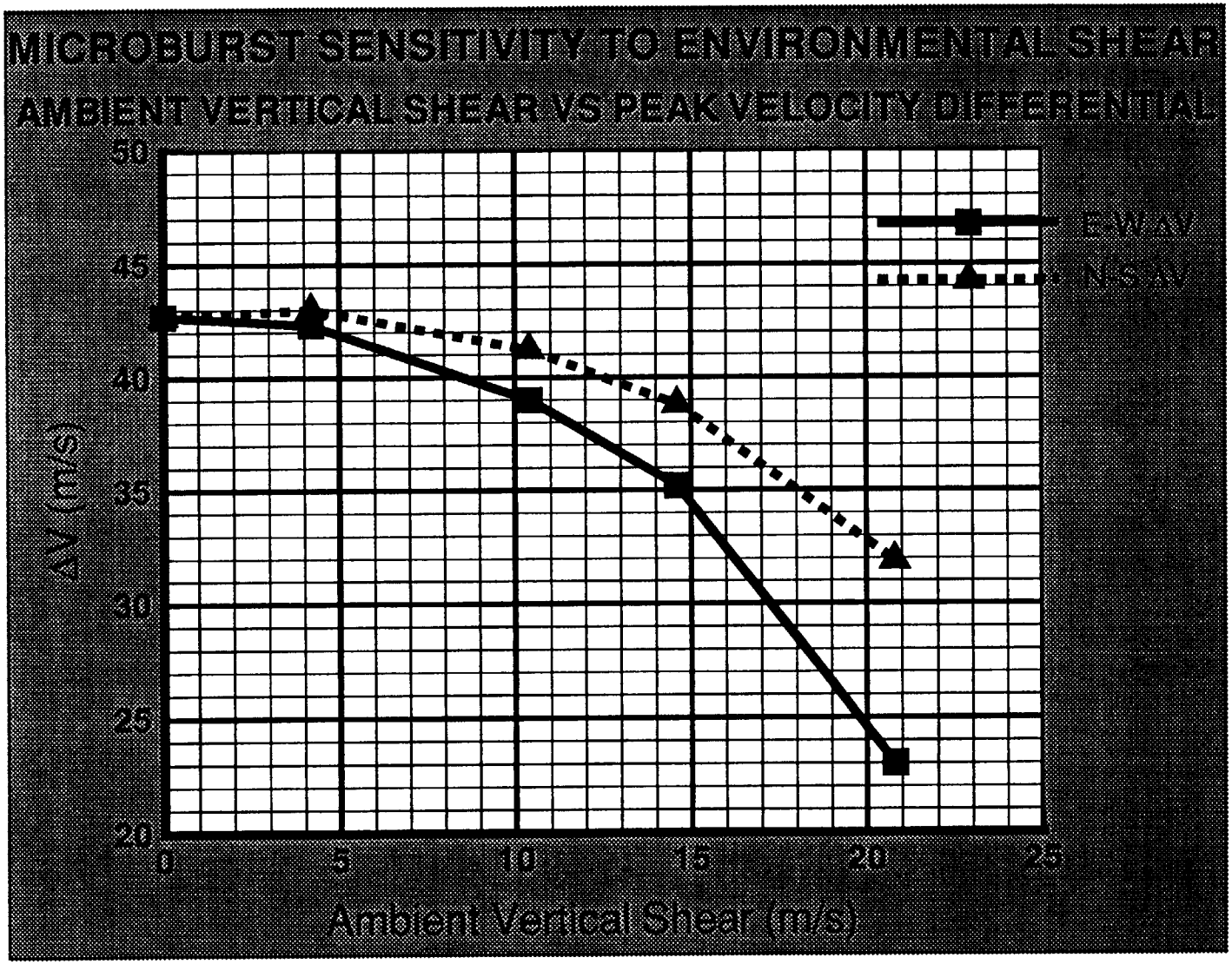
MICROBURST SENSITIVITY TO ENVIRONMENTAL SHEAR
AMBIENT VERTICAL SHEAR VS PEAK VELOCITY DIFFERENTIAL
50
45
40
35
30
25
20
ΔV (m/s)
0
5
10
15
20
25
Ambient Vertical Shear (m/s)
E-W ΔV
N-S ΔV

MICROBURST SENSITIVITY TO ENVIRONMENTAL SHEAR
AMBIENT VERTICAL SHEAR VS PEAK 1-KM AVG F-FACTOR
1-KM AVG F-FACTOR
Ambient Vertical Shear (m/s)
35
30
25
20
15
0
5
10
15
20

MICROBURST SENSITIVITY TO ENVIRONMENTAL SHEAR
AMBIENT VERTICAL SHEAR VS PEAK OUTFLOW SPEED
SDam
LDam
PEAK WINDSPEED (m/s)
40
35
30
25
20
0
5
10
15
20
25
Ambient Vertical Shear (m/s)

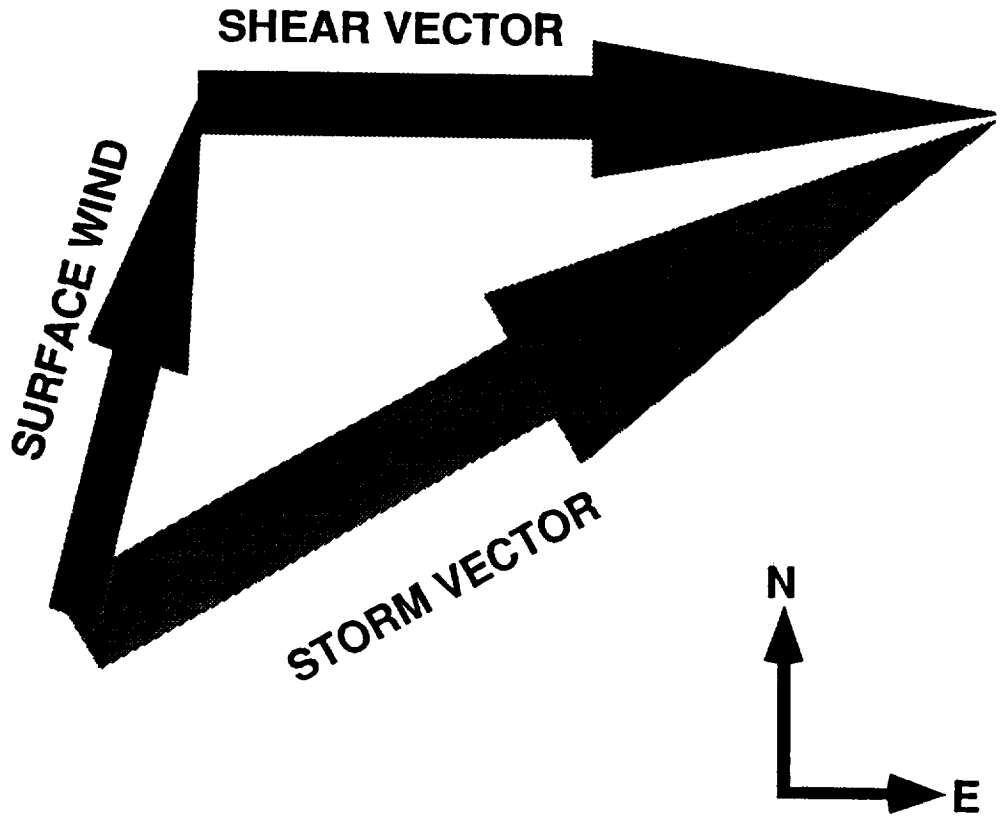


**MICROBUST PEAK WIND DIFFERENTIAL AND PEAK F-FACTOR ARE FOUND IN DIRECTION NORMAL TO SHEAR VECTOR**

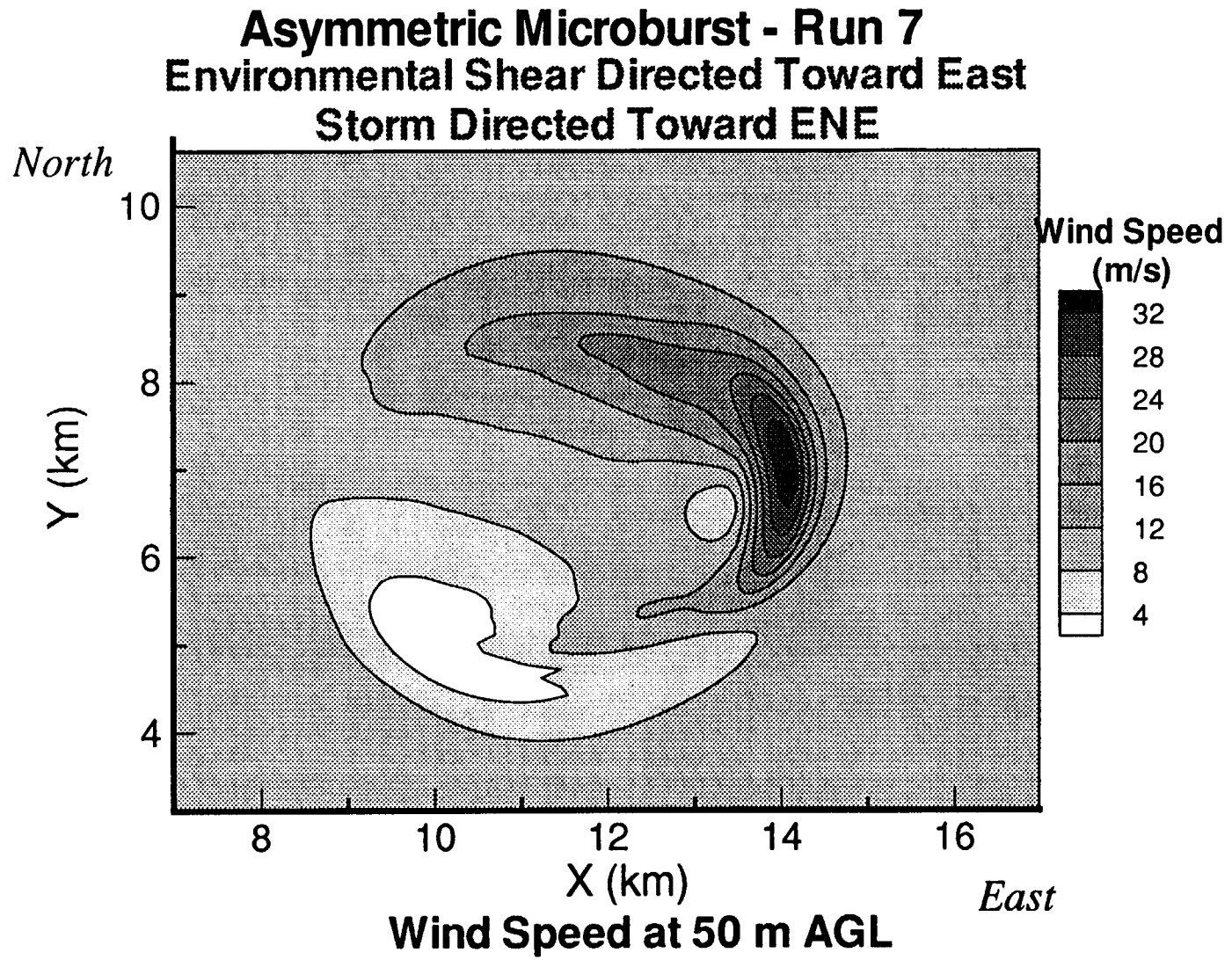
Asymmetric Microburst - Run 7
Environmental Shear Directed Toward East
Storm Directed Toward ENE
North
10
8
6
4
Y (km)
8
10
12
14
16
X (km)
East
Wind Speed
(m/s)
32
28
24
20
16
12
8
4
Wind Speed at 50 m AGL

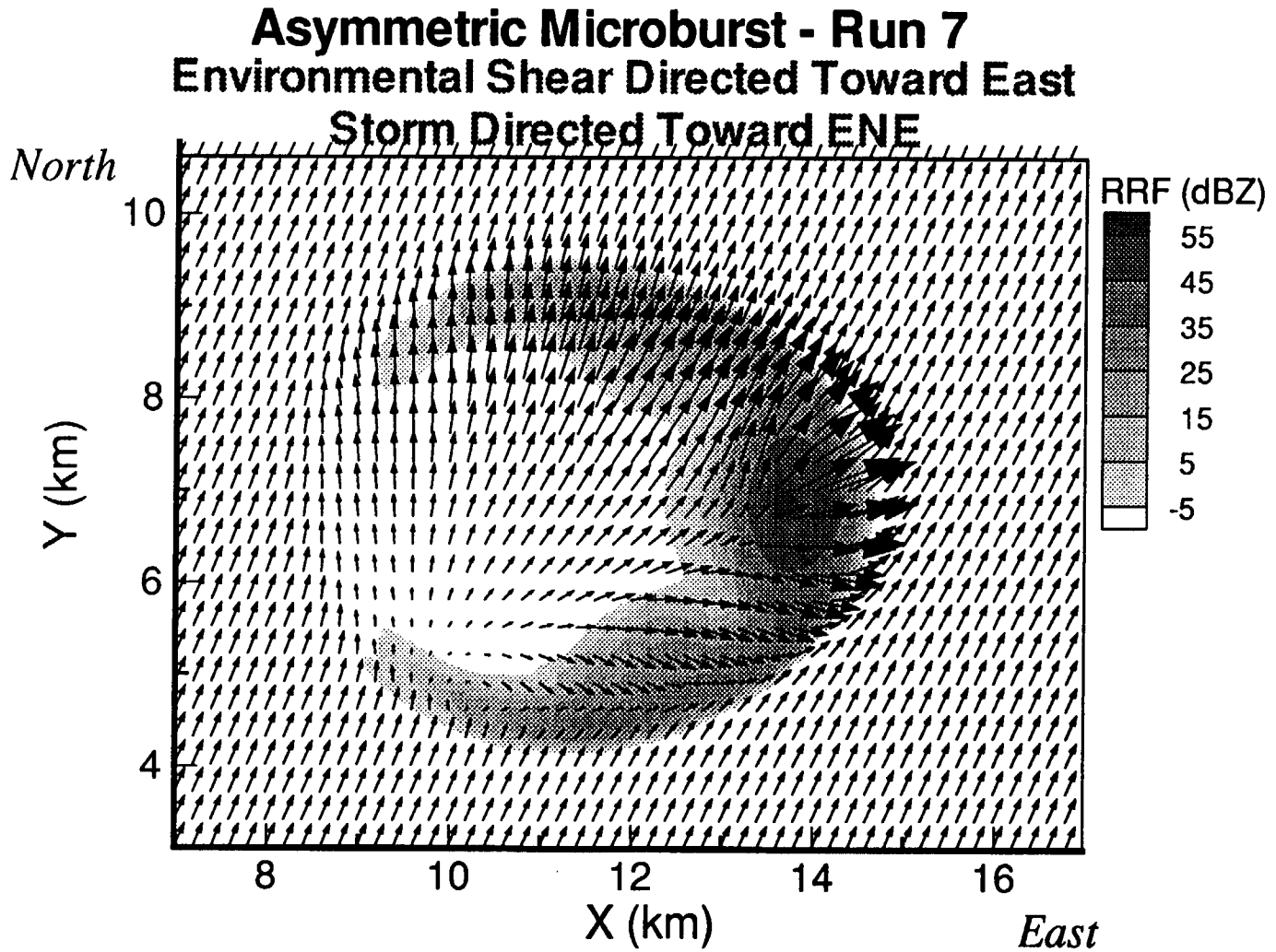
Asymmetric Microburst - Run 7
Environmental Shear Directed Toward East
Storm Directed Toward ENE
North
10
8
6
4
Y (km)
8
10
12
14
16
X (km)
East
RRF (dBZ)
55
45
35
25
15
5
-5
Radar Reflectivity and Wind Vectors at 50 m AGL

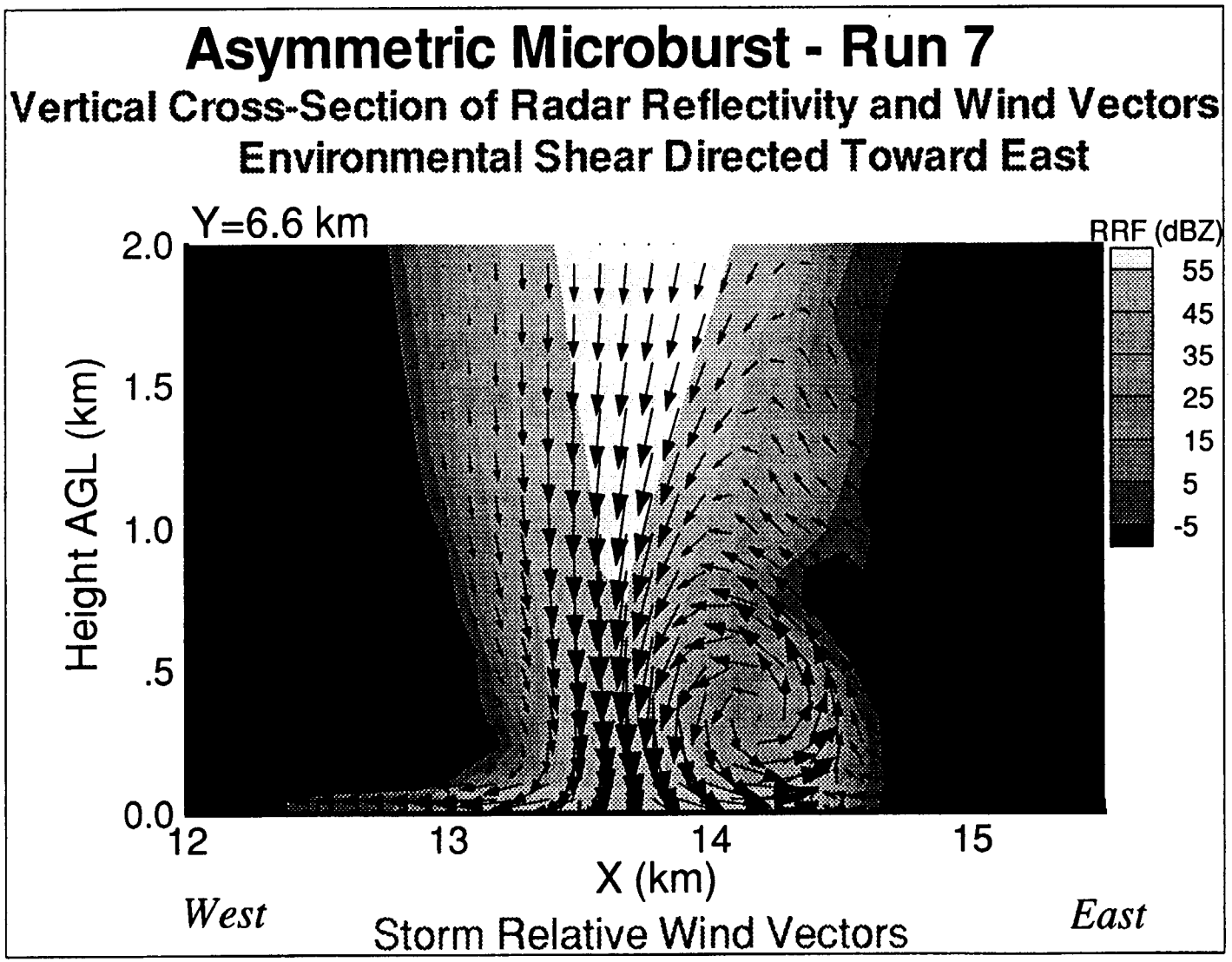
Asymmetric Microburst - Run 7
Vertical Cross-Section of Radar Reflectivity and Wind Vectors
Environmental Shear Directed Toward East
Y=6.6 km
RRF (dBZ)
55
45
35
25
15
5
-5
Height AGL (km)
2.0
1.5
1.0
.5
0.0
12
13
14
15
X (km)
West
East
Storm Relative Wind Vectors

# SUMMARY: EFFECTS OF ENVIRONMENTAL SHEAR ON MICROBURSTS

- HORIZONTAL VELOCITY DIFFERENTIAL AND F-FACTOR STRONGEST IN DIRECTION ORTHOGONAL TO ENVIRONMENTAL SHEAR VECTOR; WEAKEST IN DIRECTION OF SHEAR VECTOR
- OUTFLOW ELONGATED IN DIRECTION OF ENVIRONMENTAL SHEAR VECTOR. THE STRONGER THE SHEAR VECTOR THE GREATER THE ASYMMETRY
- VORTEX RING AND ASSOCIATED UPDRAFT INTENSIFIED ON DOWNSHEAR SIDE OF MICROBURST - BUT WEAKENED ON UPSHEAR SIDE
- OUTFLOW DEEPEST DOWNSHEAR OF DOWNDRAFT - MOST SHALLOW UPSHEAR OF DOWNDRAFT
- STRONGEST HORIZONTAL WIND SPEEDS AND GREATEST POTENTIAL FOR DAMAGING WINDS DOWNSHEAR OF DOWNDRAFT -- OPTIMAL FOR AMBIENT VERTICAL SHEAR OF 15 M/S

# NUMERICAL SIMULATION OF A PULSATING, LOW-REFLECTIVITY MICROBURST EVENT

FRED H. PROCTOR

*NASA-LANGLEY RESEARCH CENTER*
Flight Management Division
*HAMPTON, VA 23681-0001*



September 28, 1993

FIFTH COMBINED MANUFACTURERS' AND TECHNOLOGISTS'
WIND SHEAR REVIEW MEETING

# OUTLINE

I. OBSERVED CHARACTERISTICS OF DENVER, 8 JULY 1989 MICROBURST EVENT

II. INITIAL CONDITIONS FOR 3-D SIMULATION

III. RESULTS OF 3-D CASE STUDY

- A. COMPARISON WITH LLWAS
- B. DESCRIPTION OF MICROBURST EVOLUTION
- C. DESCRIPTION OF INSECT MODEL
- D. DISCUSSION OF RESULTS

IV. SUMMARY

# DENVER, 8 JULY 1989, CASE STUDY

## OBSERVED MICROBURST CHARACTERISTICS

- O Very Large Velocity Change (95 knots) Estimated From LLWAS
- O No Rain Observed, Although Blowing Dust Present
- O Not Detected by NCAR Research Radar
- O Encountered By a Boeing 737 in a "Go Around Configuration"; Reported Considerable Airspeed and Altitude Loss
- O LLWAS Data Indicated Three Major Pulses in Microburst Intensity

# Denver, 8 July 1989, Simulation

## *INPUT DATA / ASSUMPTIONS*

PHYSICAL DOMAIN SIZE
- O HORIZONTAL (X,Y): 16 KM x 16 KM
- O VERTICAL (Z): 13 KM

COMPUTATIONAL RESOLUTION
- O HORIZONTAL - 160 M (102 X 102 GRID POINTS)
- O VERTICAL - 70 M NEAR GROUND STRETCHING TO 365 M AT 13 KM (62 LEVELS)

CONVECTION INITIATED AT MODEL TIME ZERO
- O SPHEROIDAL THERMAL IMPULSE
- O DIMENSIONS - 5 KM HORIZONTAL x 2.5 KM VERTICAL
- O AMPLITUDE - $1.5^{O}$

MODEL INPUT SOUNDING
- O OBSERVED AT DENVER, 0000 UTC -- LESS THAN AN HOUR AFTER THE DEVELOPMENT OF THE STORM

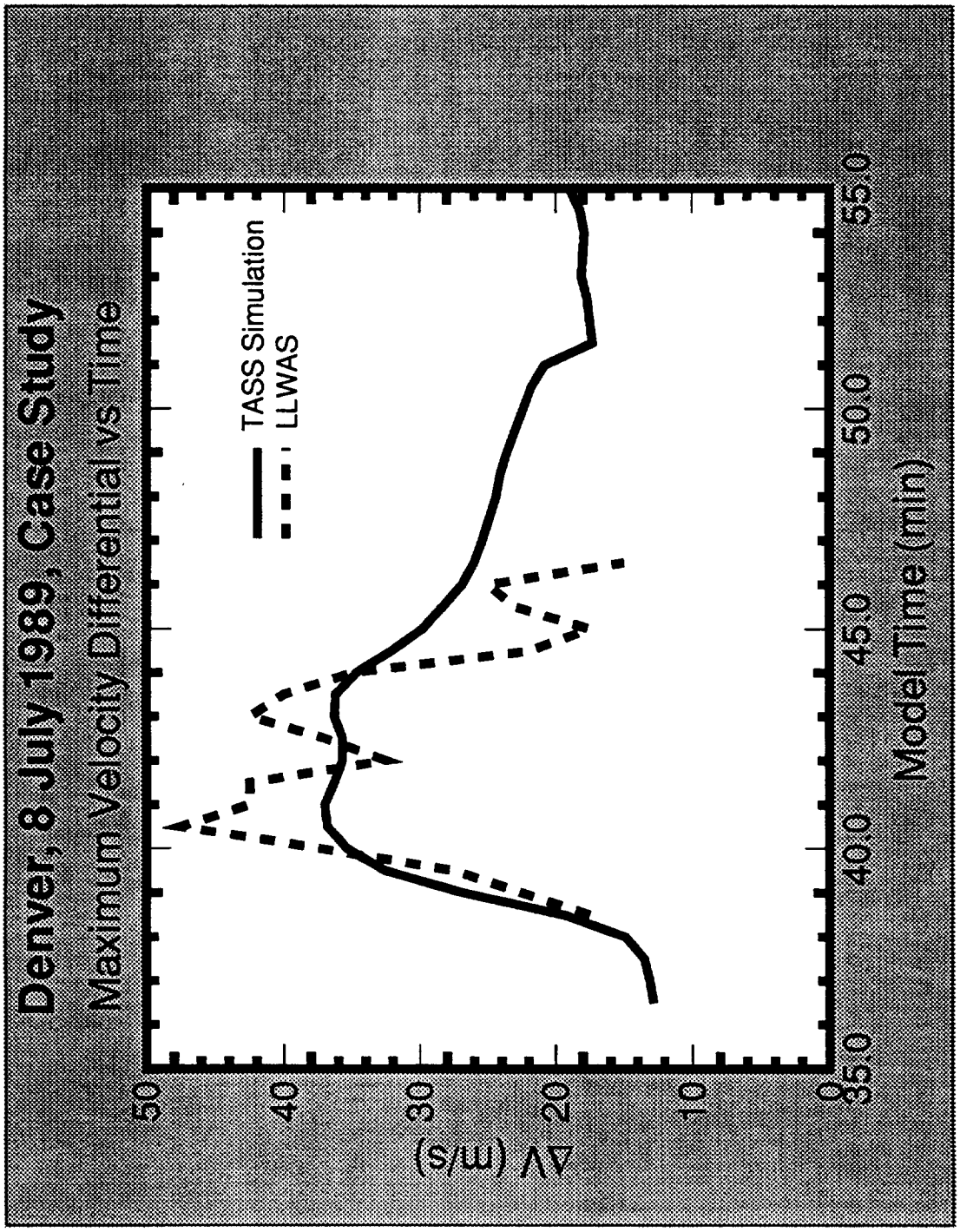
Denver, 8 July 1989, Case Study
Maximum Velocity Differential vs Time
TASS Simulation
LLWAS
ΔV (m/s)
Model Time (min)
35.0
40.0
45.0
50.0
55.0
10
20
30
40
50

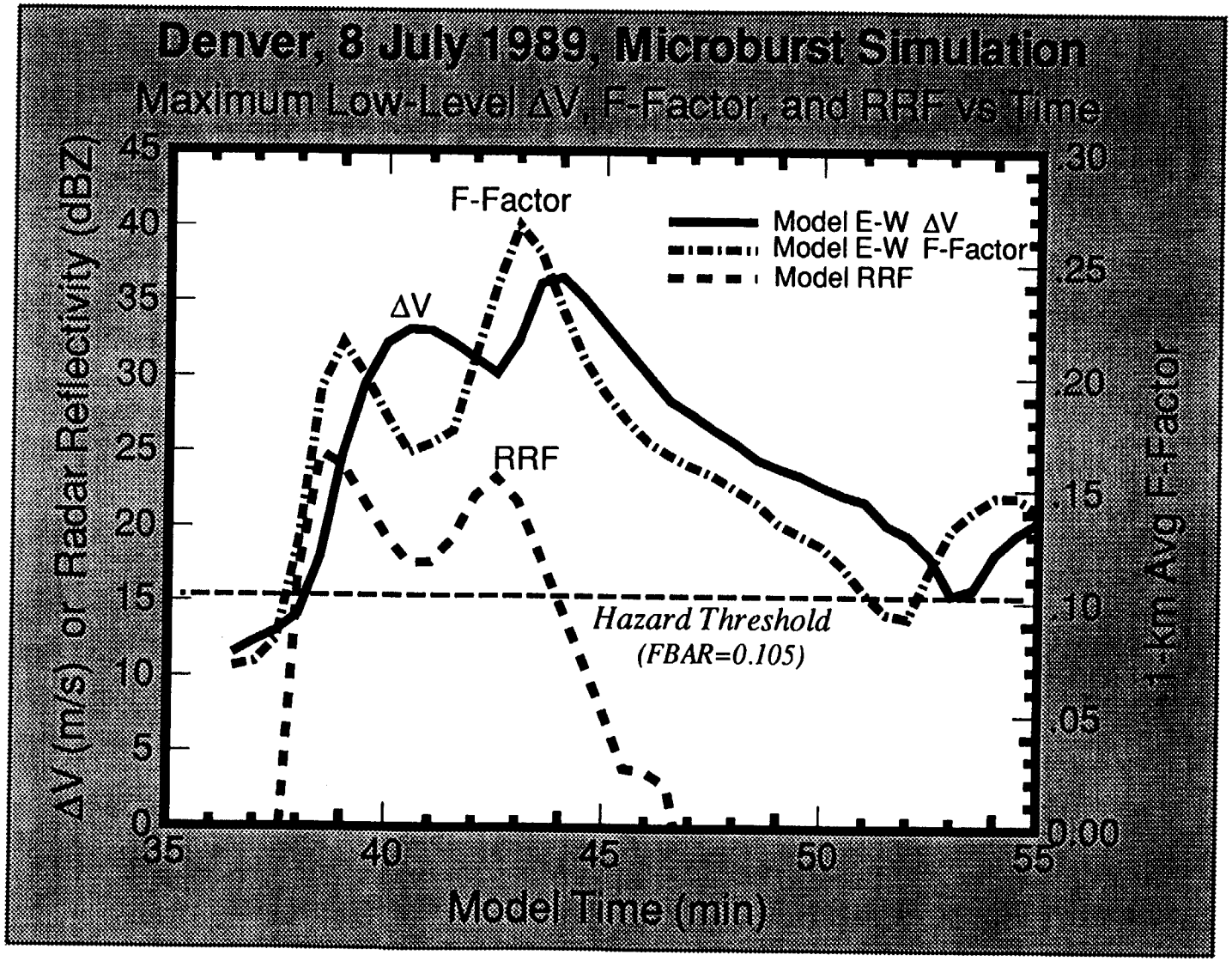
Denver, 8 July 1989, Microburst Simulation
Maximum Low-Level ΔV, F-Factor, and RRF vs Time
ΔV (m/s) or Radar Reflectivity (dBZ)
1-km Avg F-Factor
Model Time (min)
F-Factor
ΔV
RRF
Model E-W ΔV
Model E-W F-Factor
Model RRF
Hazard Threshold
(FBAR=0.105)
0
5
10
15
20
25
30
35
40
45
.00
.05
.10
.15
.20
.25
.30
35
40
45
50
55

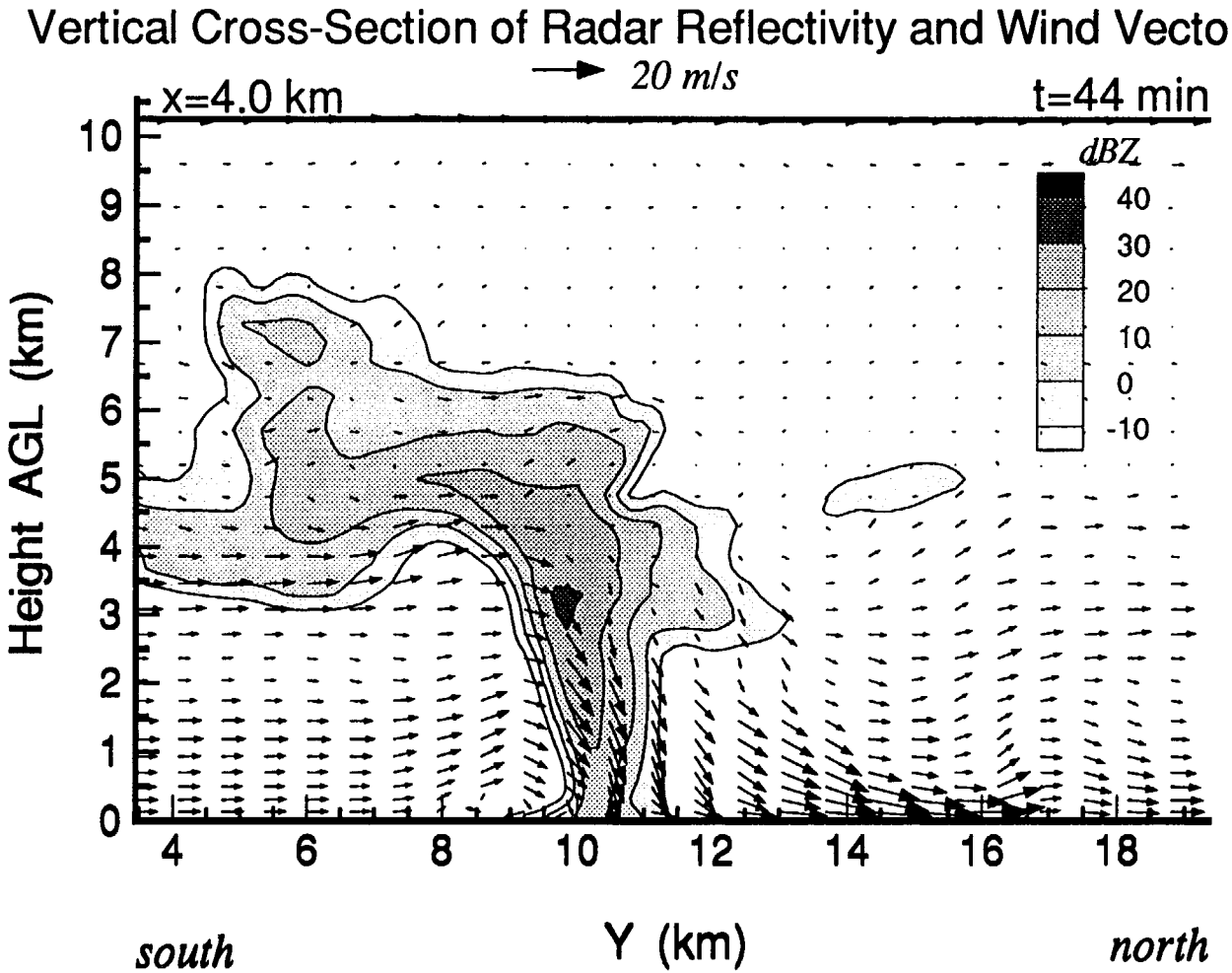
Vertical Cross-Section of Radar Reflectivity and Wind Vectors
20 m/s
x=4.0 km
t=44 min
dBZ
40
30
20
10
0
-10
Height AGL (km)
0
1
2
3
4
5
6
7
8
9
10
4
6
8
10
12
14
16
18
south
Y (km)
north

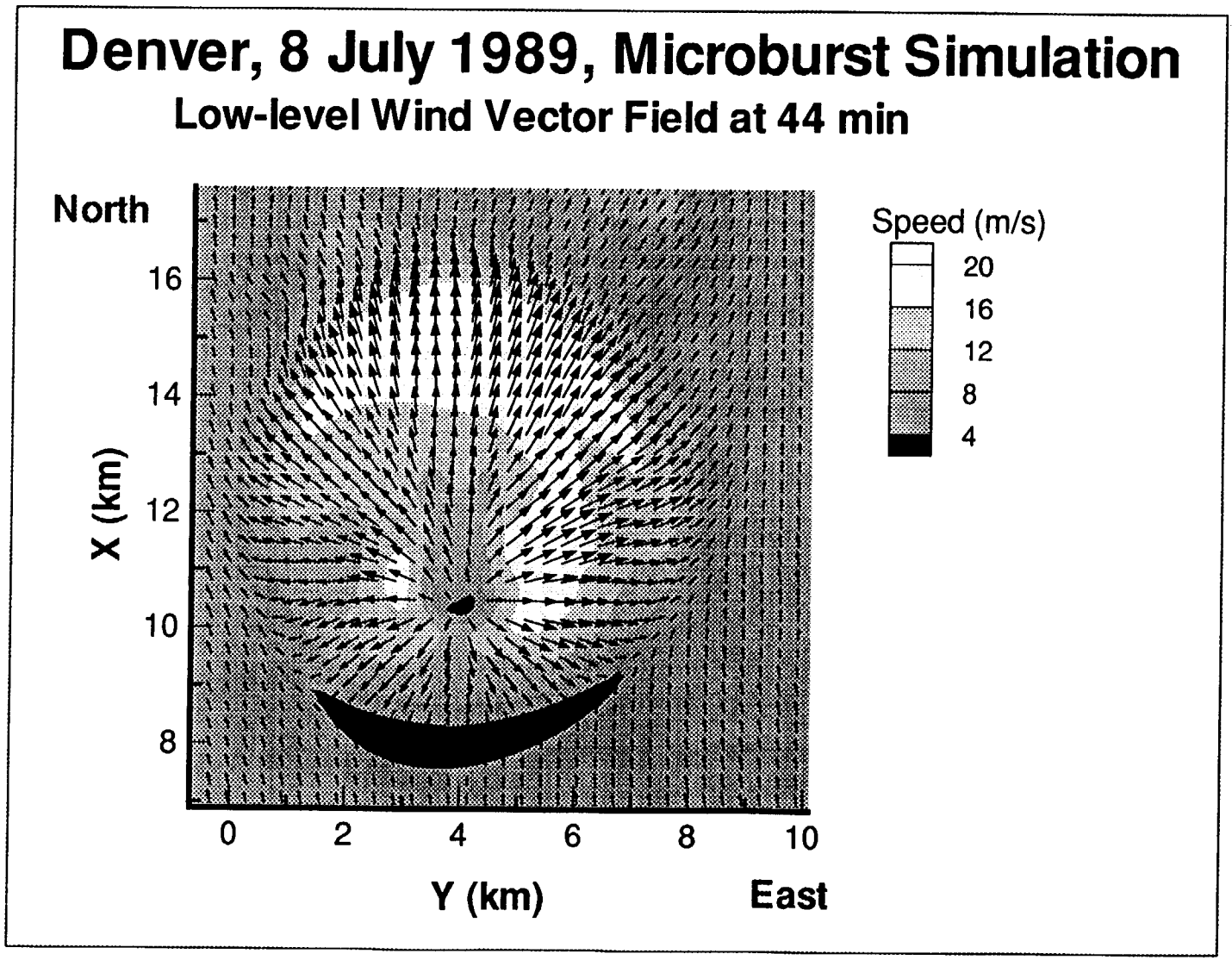
Denver, 8 July 1989, Microburst Simulation
Low-level Wind Vector Field at 44 min
North
16
14
12
10
8
X (km)
0
2
4
6
8
10
Y (km)
East
Speed (m/s)
20
16
12
8
4

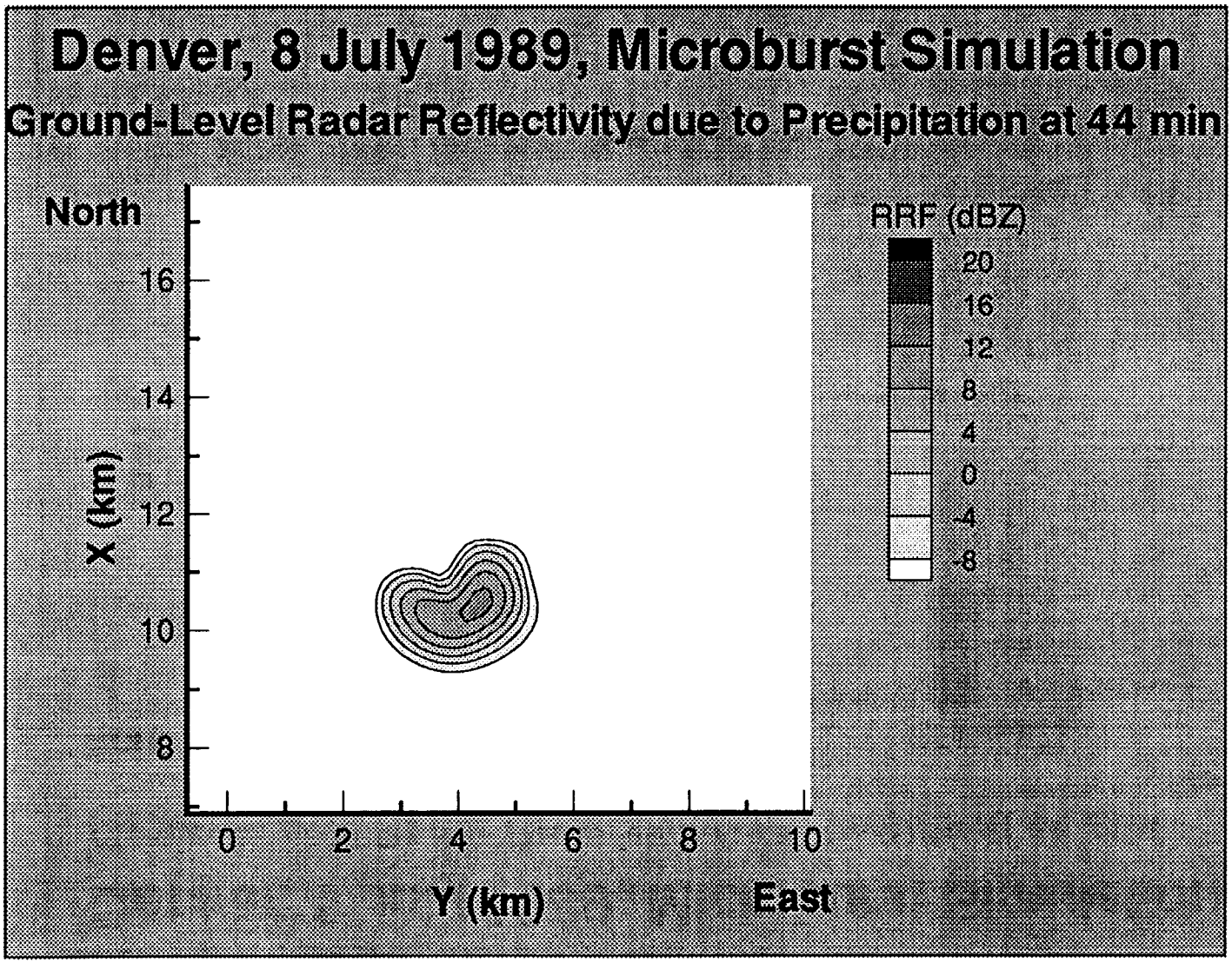
Denver, 8 July 1989, Microburst Simulation
Ground-Level Radar Reflectivity due to Precipitation at 44 min
North
X (km)
16
14
12
10
8
0
2
4
6
8
10
Y (km)
East
RRF (dBZ)
20
16
12
8
4
0
-4
-8

# Denver, 8 July 1989, Microburst Simulation

## Ground-Level Radar Reflectivity with insects at 44 min

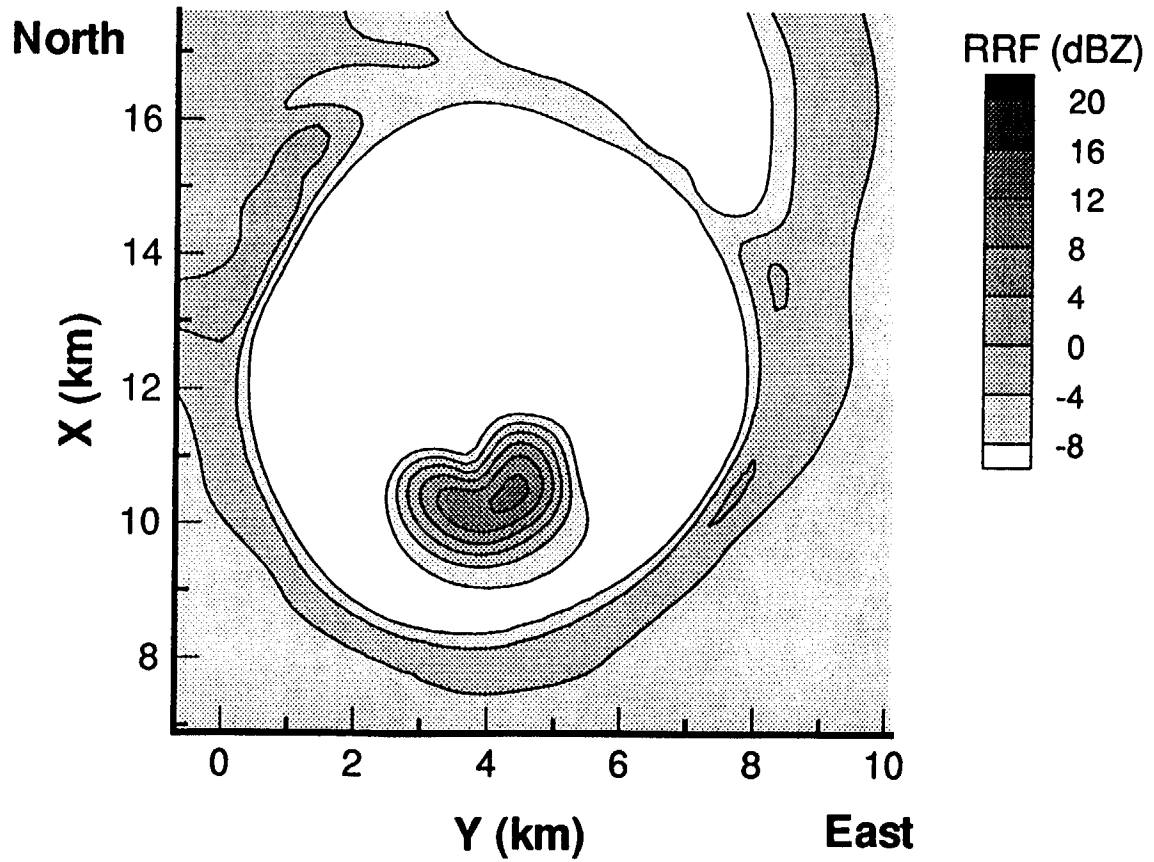

# Denver, 8 July 1989, Microburst Simulation

## North-South F-Factor at 44 min and 150 m AGL

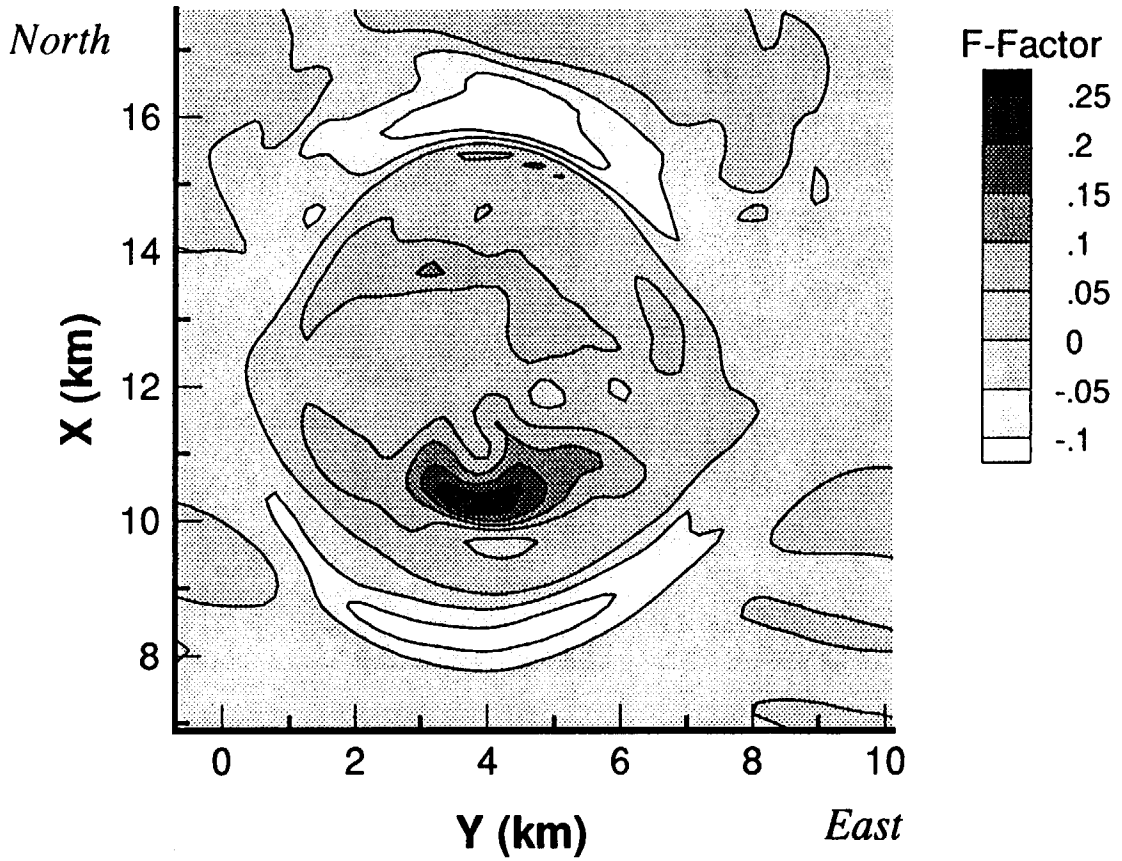

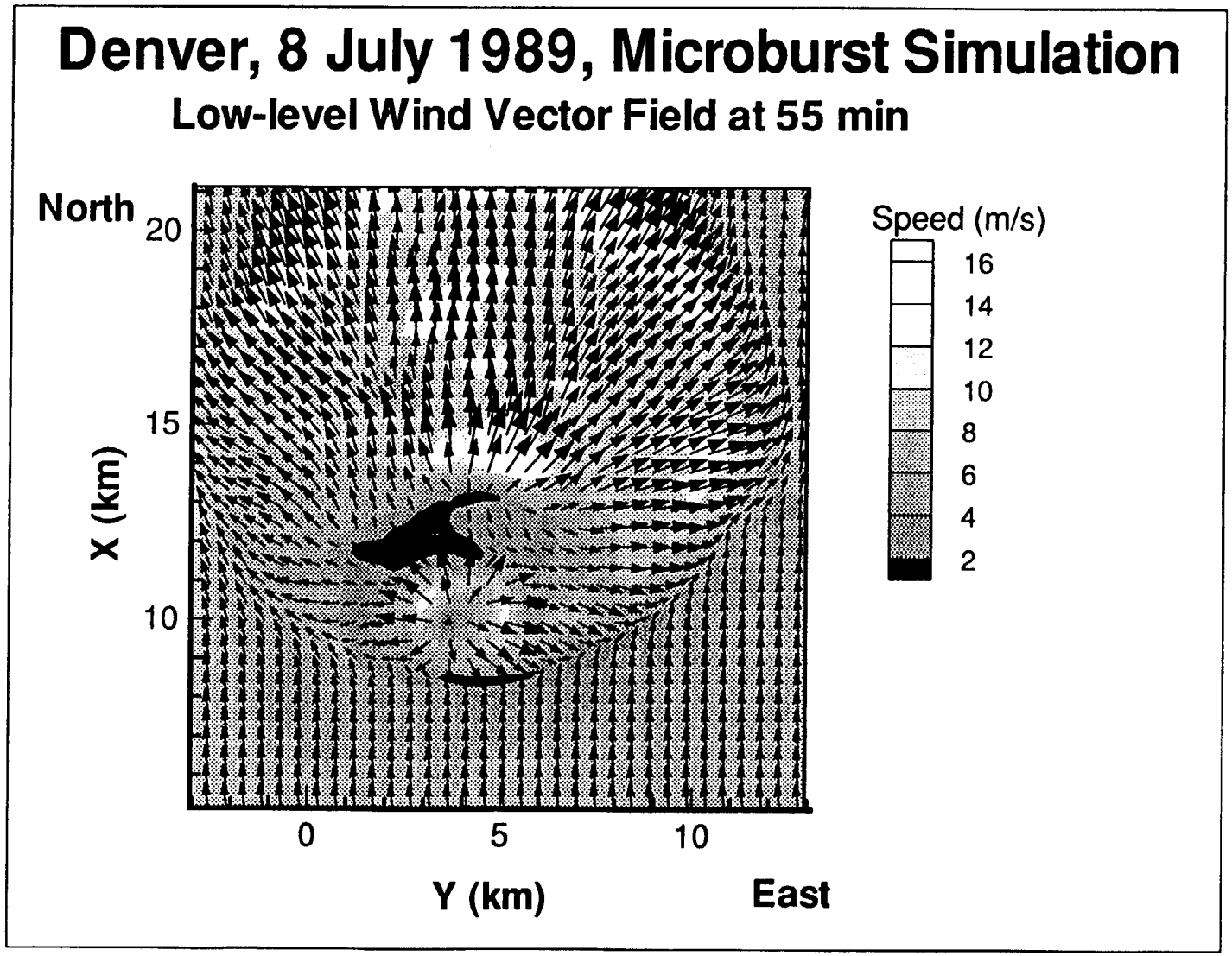
Denver, 8 July 1989, Microburst Simulation
Low-level Wind Vector Field at 55 min
North
20
15
10
X (km)
0
5
10
Y (km)
East
Speed (m/s)
16
14
12
10
8
6
4
2

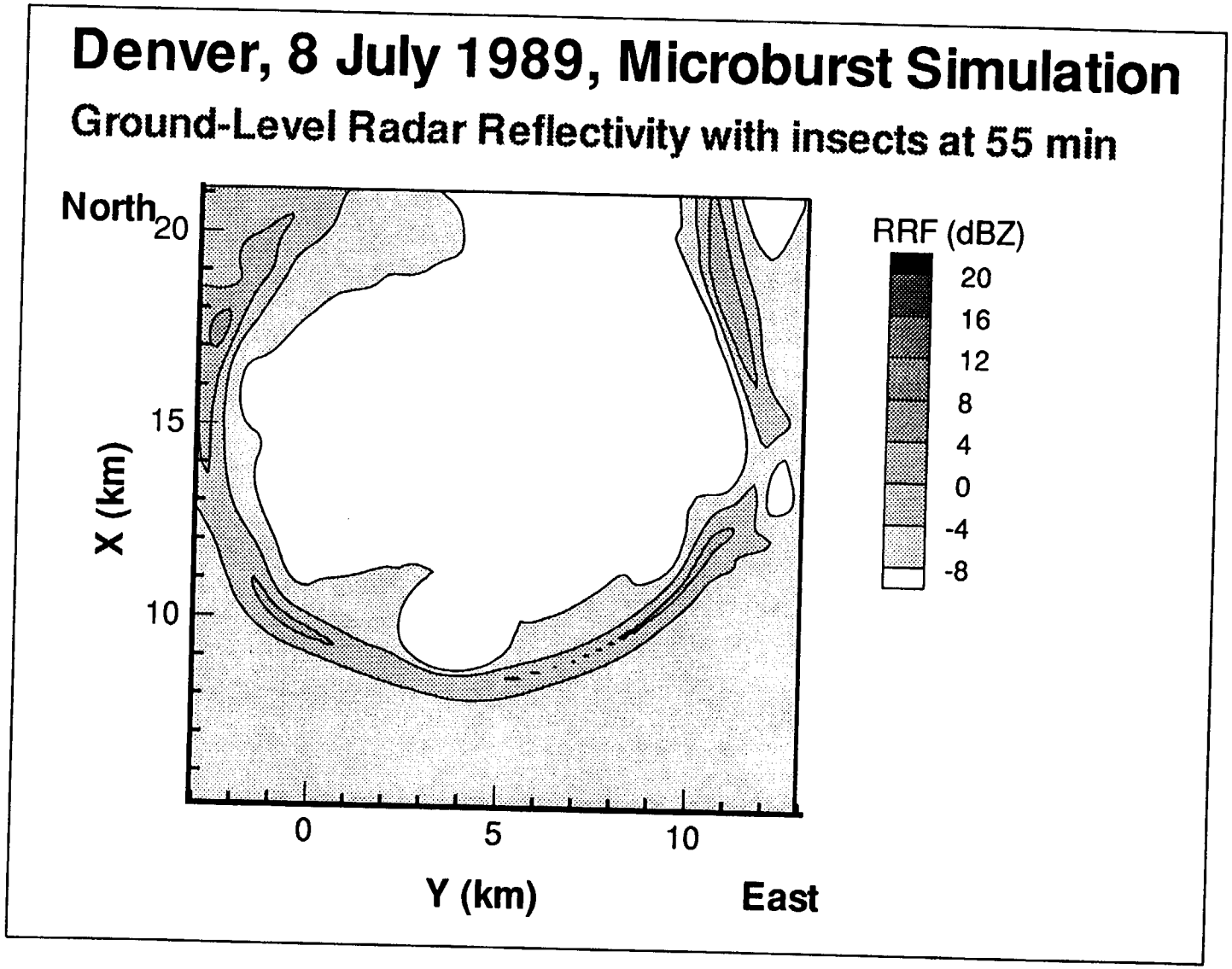
Denver, 8 July 1989, Microburst Simulation
Ground-Level Radar Reflectivity with insects at 55 min
North
20
15
10
X (km)
0
5
10
Y (km)
East
RRF (dBZ)
20
16
12
8
4
0
-4
-8

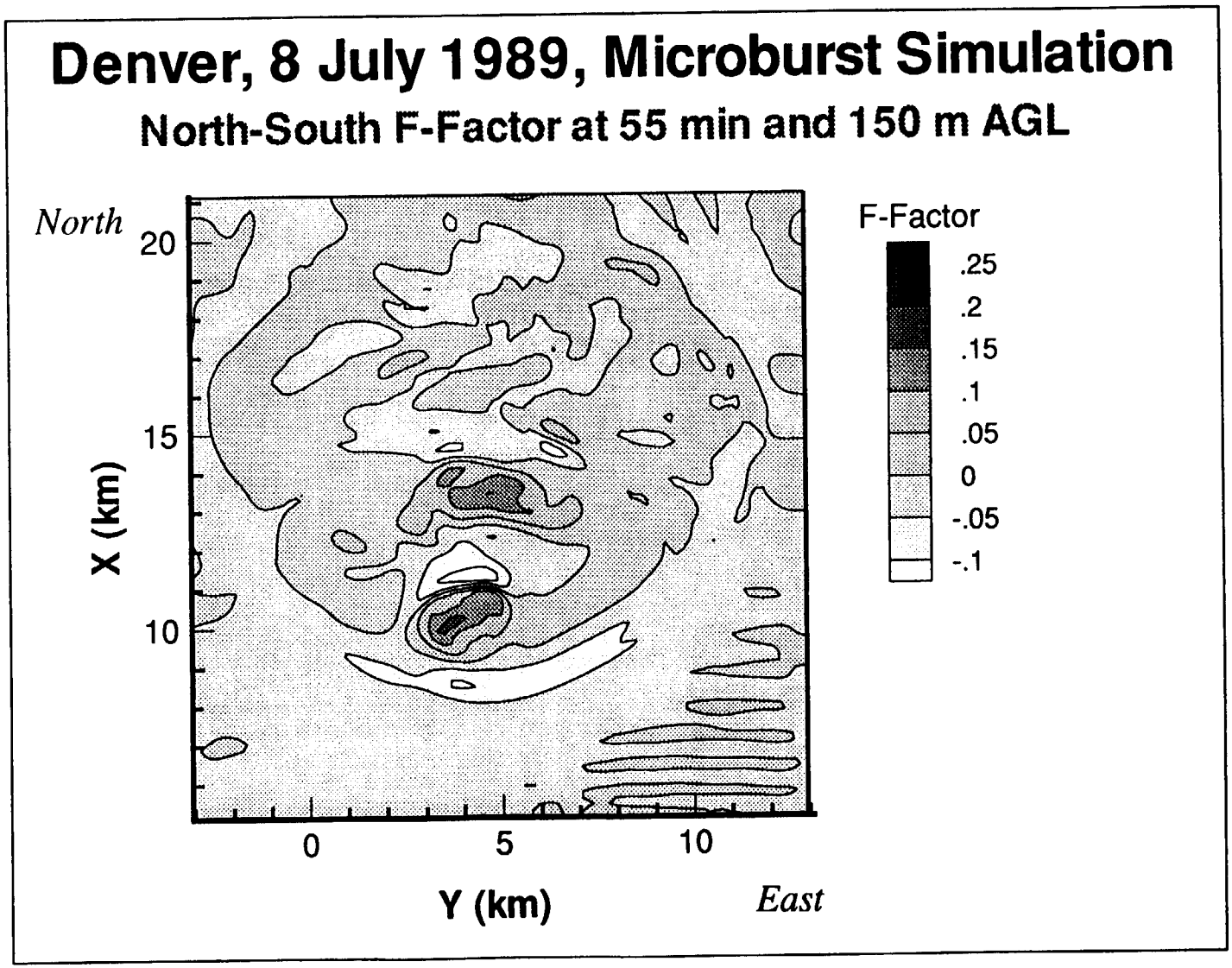
Denver, 8 July 1989, Microburst Simulation
North-South F-Factor at 55 min and 150 m AGL
North
20
15
10
X (km)
0
5
10
Y (km)
East
F-Factor
.25
.2
.15
.1
.05
0
-.05
-.1

# SUMMARY OF MODEL SIMULATION

- LOW REFLECTIVITY MICROBURST WITH HAZARDOUS WIND SHEAR
- THREE DISTINCT MICROBURST PULSES OVER 20 MINUTE PERIOD
- VIRGA FROM DISSIPATING PARENT CLOUD MAINTAINS HAZARDOUS WINDSHEAR FOR PERIOD MUCH LONGER THAN TYPICAL MICROBURST LIFETIME
- PRECIPITATION REACHES GROUND ONLY DURING THE FIRST FEW MINUTES OF THE EVENT -- MOST OF OUTFLOW CONTAINS NO PRECIPITATION
- THE CONTRIBUTION TO RADAR REFLECTIVITY FACTOR FROM INSECTS IS GREATEST IN CONVERGENT AREAS, SUCH AS ALONG BURST FRONT
- MICROBURST DOWNDRAFTS TRANSPORT INSECT-FREE AIR FROM ABOVE THE PLANETARY BOUNDARY LAYER., RESULTING IN MINIMAL INSECT CONCENTRATIONS WITHIN WINDSHEAR HAZARD AREAS.
- SOME LOW-REFLECTIVITY MICROBURST EVENTS MAY BE DIFFICULT TO DETECT WITH RADAR DUE TO LACK OF BOTH PRECIPITATION AND INSECTS

# INSECT MODEL

## ASSUMPTIONS

- O Monodispersive Size Distribution
- O Horizontal Translation Relative to Air Motion
- O Radar Reflectivity Factor Proportion to Number Density
- O Initialized Having a Uniform Number Density Within Boundary Layer
- O No Sources or Sinks (e.g., rainout, ground sources)
- O Fall Speed ($W_f$) a Function of Temperature (T) and Vertical Air Motion (W)
  Models observed behavior in which insects:
  1) try to maintain the same altitude in ascending air
  2) descend relative to air motion if carried to level where $T < 10^{o}C$
  3) have a maximum fall speed of 75 cm/s

# Local Number Concentration of Insects Governed by:

$$\frac{\partial N}{\partial t} = -V\cdot\nabla N + \frac{1}{\rho}\frac{\partial \rho N W_I}{\partial z} + \nabla\cdot K\nabla N$$

$$W_I = \begin{cases} W_{max} & \text{if } T < 10^oC \text{ or } W > W_{max} \\ W & \text{if } T > 10^oC \text{ and } 0 < W < W_{max} \\ 0 & \text{if } T > 10^oC \text{ and } W > 0 \end{cases}$$

where $W_{max} = 0.75$ m/s.

Based on insect behavior as reported in: *G. L. Achtemeier; The Use of Insects as Tracers for "Clear-Air" Boundary-Layer Studies by Doppler Radar, J. Atmos Oceanic Technol., 8, 1991, pp 746-765.*